Optical and Quantum Electronics (2020) 52:177, https://doi.org/10.1007/s11082-020-02297-6

Expedient Paramagnetic Properties of Surfactant-Free Plasmonic Silicon-Based Nanoparticles

Yury V. Ryabchikov[1,2*] and Jan Behrends[3]

[1] *HiLASE Centre, Institute of Physics of the Czech Academy of Sciences, Za Radnicí 828, 25241 Dolní Břežany, Czech Republic*

[2] *P.N. Lebedev Physical Institute of the Russian Academy of Sciences, 53 Leninskii Prospekt, 119 991, Moscow, Russia*

Yury V. Ryabchikov: ORCID : 0000-0002-6844-1051

[3] *Berlin Joint EPR Lab, Fachbereich Physik, Freie Universität Berlin, Arnimallee 14, 14195 Berlin, Germany*

Jan Behrends: ORCID: 0000-0003-1024-428X

ABSTRACT

Surfactant-free multifunctional semiconductor-metallic nanostructures possessing several modalities are formed due to laser-induced structural modification of pure silicon nanoparticles in the presence of gold. It results to variable size-dependent chemical composition examined by energy-dispersive X-ray spectroscopy. Laser-synthesized silicon-based nanocomposites exhibit remarkable both plasmonic and paramagnetic properties. Their plasmonic maxima are found to be easily adjusted in the whole visible spectral range. Influence of resonant laser irradiation on spin behaviour of silicon-gold nanoparticles is established. Their spin-lattice and spin-spin relaxation processes are investigated as well. Such multifunctional nanoparticles can reveal a huge potential for different applications in field of nanomedicine, in particular, for biosensing and bioimaging.

Key words: silicon nanoparticle, silicon-gold nanoparticle, nanocomposite, EPR, laser ablation, plasmonic property[†]

[*] Correspondence to: Yu.V.R. (yury.ryabchikov(at)hilase.cz, ryabchikovyv(at)lebedev.ru)

[†] *Abbreviations*: nano-Si, nanostructured silicon; Si NPs, silicon nanoparticles ; fs, femtosecond; Si@Au NPs, silicon-gold nanoparticles ; HR-TEM, high-resolution transmission electron microscopy; EDX, energy-dispersive X-ray spectroscopy; cw, continuous wave; EPR, electron paramagnetic resonance; Au_XSi_Y, gold silicide nanoformulation; P_b-center, silicon dangling bond.

Introduction

Nanostructured silicon (nano-Si) is a perspective material due to its unique optoelectronic properties, resulting in potential applications in photovoltaics [1–6], nanothermometry [7–9], or nanoscale electronic devices [10,11]. Meanwhile, one of the most appealing prospects is related to the field of nanomedicine, in particular to drug delivery, singlet oxygen generation, magnetic resonance and optical bioimaging as well as cancer treatment [12–30].

Particularly promising are silicon nanoparticles (Si NPs) prepared by means of pulsed laser ablation in liquid, revealing several aspects important for biomedical applications [12,30–35]. Indeed, such a method allows formation of biocompatible nanomaterials due to the use of contamination-free conditions. Recently it was shown that the functionality of Si NPs can be significantly extended due to combination of specific properties of nanostructured silicon and gold incorporated in one composite nanoparticle [36–38]. However, investigation of formation mechanisms, properties and applications of laser-synthesized semiconductor-metallic composite NPs just started to attract research interest lately and is on its early stage [36–42].

In this work, the formation of plasmonic composite silicon-gold nanoparticles (Si@Au NPs) with size-dependent chemical content by means of laser-induced structural modification of Si NPs is carried out. A method for adjusting the position of the plasmonic resonance in the visible spectral range is developed. The impact of structural modification of the laser-synthesized Si-based NPs on their defect structure is investigated. The influence of laser irradiation (532 nm) on spin behaviour as well as spin-lattice and spin-spin relaxation processes are studied.

Experiments

Composite silicon-gold nanoparticles are formed by 2-step approach based on pulsed laser ablation in liquid method. Firstly, Si NP colloidal solution is synthesized by laser ablation of a silicon wafer (p-type, (100), 10 Ω·cm) immersed in deionized water (18 MΩ·cm). As a second step, laser ablation of a gold target (Goodfellow, 99,99 % purity) in previously-prepared colloidal

solution of Si NPs is carried out. In both cases, a Ti:sapphire femtosecond (150 fs) laser (Astrella, Coherent) operated at 800 nm wavelength with 1000 Hz repetition rate is used. Laser radiation of 150 μJ/pulse fluence is focused by a 75 mm lens on a solid target surface. Duration of laser treatment of the targets in each case is 30 minutes. More detailed information related to synthesis of composite nanoparticles is published elsewhere [36,37]. The use of substances of high purity accompanied by laser irradiation leads to the first important modality of Si@Au NPs – ***biocompatibility***.

Their structural properties are studied by means of a high-resolution transmission electron microscope (HR-TEM) using a carbon-coated copper grid containing some amount of NPs. A calculation of the NP size distribution is carried out by the Image J software. The chemical composition of the NPs is investigated with the help of a microscope coupled to an Energy Dispersive X-ray (EDX) spectroscopy system choosing a single NP of a given size. Size-dependent mass contribution of silicon and gold species in composite NPs of different sizes is estimated.

The optical properties of the Si-based NPs are studied by means of a Shimadzu UV-2600 spectrophotometer. Continuous wave (cw) and pulsed electron paramagnetic resonance (EPR) measurements are carried out on a Bruker ELEXSYS E580 EPR spectrometer operating at X band (~9.8 GHz frequency) using a field modulation amplitude of 0.5 mT (in the cw EPR measurements). The light-induced properties of paramagnetic states are investigated by irradiating the samples in the resonator by a laser diode (532 nm, 10 mW). Defect concentrations for the Si-based nanoparticles were determined by quantitative EPR measurements as described earlier [43].

Results

A TEM image of multicomponent Si@Au nanoparticles is presented in Fig. 1a showing NPs of different shapes (predominately spherical-like). Calculated size distribution is found to be very narrow (~ 5 nm) with an average size 7 – 8 nm (Fig. 1b). One can see that this size distribution is significantly reduced due to laser-induced treatment compared to that of initial Si NPs. Indeed, mean size of single-component NPs is 30 nm with size dispersion ~ 20 nm (Fig. 1b). Performed

calculation reveals that majority of NPs (~ 95 – 97 %) possess diameter beyond 10 nm (Fig. 1c) while minority of them (~ 3 – 5 %) has size up to 100 nm (Fig. 1d). The small (10 nm) and large (100 nm) composite NPs may reveal different structure and chemical composition. For instance, small NPs may combine nanocristalline and amorphous phases of Si (responsible for Raman and EPR signals [31], respectively) with nanocristalline gold. Performed calculation of interatomic distances in a small NP (Fig. 1c) shows the following value (2.36 Å) that corresponds to (111) atomic plane of gold. In order to study chemical composition of individual nanoparticles, EDX study by means of HR-TEM is carried out.

In Fig. 2a, an EDX spectrum of a 7 nm multifunctional Si@Au NP is shown. The spectrum reveals several maxima at different energy positions. Here, responses at 0.26 keV and 0.9 keV/8.0 keV/8.9 keV correspond to K_α of carbon and $L_\alpha/K_\alpha/K_\beta$ lines of copper, respectively, originating from a used copper TEM grid covered with a carbon film. The signals at 2.1 keV and 9.7 keV are related to M_α and L_α lines of gold, respectively. K_α line of silicon at 1.7 keV suggests the presence of Si in the NP composition. It worth noting that peak intensity is proportional to the mass fraction of the element concerned. Hence, an EDX spectrum of Si@Au NPs with equal amount of silicon and gold atoms will reveal higher intensity for a gold peak due to 7-times higher mass in comparison with silicon.

One can see that the mass contribution of the different elements strongly depends on the diameter of the composite NPs (Fig. 2b). Indeed, the size-dependent chemical composition of Si@Au NPs is found to be divided into two different specific regions (Fig. 2b). Firstly, small (less than 10 nm) NPs have a content remarkably changing with their size. Here, mass contribution of gold in Si@Au NPs increases with NP size. These data (Fig. 2b) allow estimating a mass ratio between different elements for a NP of a given size. So far as gold possesses 7-times higher mass than silicon, number of atoms of different elements will significantly differs for small and large NPs. Indeed, 27/73 Si/Au mass ratio of a 7 nm composite NP results in 72/28 Si/Au atomic ratio showing predominant content of Si atoms in the composite NP [36]. Such NPs are named as Si@Au

NPs in contrast to Au@Si NPs possessing higher amount of gold atoms. Indeed, according to the EDX study, Au@Si NPs (size more than 20 nm) have 22/78 Si/Au atomic ratio (or 3/97 Si/Au mass ratio) [36]. This data clearly shows a ***multicomponent modality*** with ***tuned chemical composition*** of NPs formed by a laser-assisted approach.

Metal content results in the appearance of a new functionality unique for Si-based NPs – ***plasmonic properties***. Indeed, a clear plasmonic maximum at 520 nm (Fig. 3a) is found in composite NPs due to a presence of nanostructured gold (Fig. 2a) incorporated into the Si NPs. It is worth noting that the position can be easily adjusted in the whole visible spectral range by using an appropriate metal target for synthesis of the composite NPs (Fig. 3a, inset).

The presence of silicon shows the forth modality of Si@Au NPs – a substantial concentration of ***paramagnetic states***. It is reflected in a strong isotropic single-component EPR signal of Si@Au NPs with full width of half maximum of 7 G that is very similar to a spectrum of initial pure Si NPs (Fig. 3b). Absorption spectra and double integral curves of Si-based NPs are shown in inset and allow estimating the defect concentration based on quantitative EPR measurements. The EPR spectrum of Si@Au NPs is approximately 5 times lower than that of Si NPs. This indicates that the composite nanoparticles have a lower number of paramagnetic states. Indeed, the estimated defect concentration of Si@Au NPs is $0.47 \cdot 10^{19}$ spin/g while pure Si NPs possess $2.21 \cdot 10^{19}$ spin/g. Additionally, an impact of a green illumination (resonant for Si@Au NPs) on the concentration of unpaired electrons in Si-based NPs is studied. Corresponding results are also shown in Fig. 3b. Here, lines indicate EPR spectra of Si-based NPs obtained in the dark while open points present the EPR spectra under the green illumination. However, they reveal no any changes in concentration of spins for both types of laser-synthesized Si-based NPs contrary to counterparts prepared by electrochemical etching method [19]. Moreover, study by means of pulsed EPR shows complete absence of any spin echo signals of the laser-synthesized NPs in temperature range between 20 and 300 K.

Discussion

Irradiation of materials immersed in a liquid with a pulsed laser leads to strong laser-matter interaction involving numerous interrelated processes [44–50]. As a result, laser-synthesized NPs are formed with the properties considerably dependent on experimental conditions. In particular, semiconductor-metallic NPs can be synthesized due to laser ablation of a metal target immersed in a colloidal solution containing semiconductor NPs [36–38]. In this case, the following processes take place:

1) laser ablation of a metal target where the laser energy is absorbed by the free electrons of metal (inverse bremsstrahlung);
2) laser fragmentation of Si NPs where the laser energy is primarily absorbed by the valence electrons, leading to their excitation to the conduction band followed by the inverse bremsstrahlung process.

In this study, an fs laser has been chosen in order to minimize the heat-affected zone in matters. Indeed, during the laser action the ions of the lattice in the near-surface layer of a target or NPs still remain cold [44,46] as the pulse duration (~150 fs) is much shorter than the characteristic relaxation times [44,46]. However, the electrons within the optical penetration depth that absorb light are driven to a high temperature [44]. Upon electron lattice relaxation at picosecond timescale, the material lattice is overheated to a high temperature, culminating in decomposition into a mixture of vapor and nanoclusters (phase explosion). These ablation products, containing both silicon and gold atoms, ions and nanoclusters are expanding, being however spatially confined by the surrounding liquid medium [51]. This provokes fast cooling of the ablated species leading to formation of an oscillating cavitation bubble where Si@Au NPs may be formed [52,53] as a result of interaction between silicon and gold atoms and nanoclusters. Moreover, interaction between the ablation products and liquid may result in appearance of unusual phases [47,49,50], e.g., gold silicide nanoformulations of different stoichiometry (Au_xSi_y) that will be studied additionally. It should be mentioned that the formation of NPs may also take place in the surrounding liquid

outside the cavitation bubble in the adjacent layers of liquid [49,52,54]. In this case, Au@Si NPs can be formed, small amount of which is detected during TEM study (Fig. 1d).

It worth noting that the self-focusing effect can occur due to the high value of the peak laser power. Indeed, under used experimental conditions, the estimated peak power is ~ 600 MW significantly exceeding the critical value for self-focusing (~ 3.5 MW). This can provoke filamentation of the laser beam propagating in the water-based colloidal solution through the whole liquid layer (10 mm) [55]. Hence, silicon nanoparticles can be decomposed into atomic and nanocluster phases along the laser filament, subsequently covering large Au NPs with a thin silicon shell (Fig. 1d).

The presence of 28 % of gold atoms (for a 7 nm Si@Au NP according to the EDX study) reveals remarkable plasmonic properties associated with collective oscillations of free electrons in nanostructured gold (Fig. 3a). Choosing different metals (silver, copper) with other plasmonic frequencies, one can easily adjust the position of a plasmonic maximum (Fig. 3a, inset). The plasmonic properties of the Si-based NPs reported here will promote the application of semiconductor-based NPs into biomedical-related fields, namely, for biosensing due to surface-enhancement of optical signals.

As it is shown above, the laser treatment of Si NPs leads to a significant change of their size, chemical composition and optical properties. However, the defect structure of the NPs does not change regardless of the laser-induced modification. Indeed, one can see that the EPR spectra of both single- and multicomponent Si-based NPs are identical except for the signal amplitude (Fig. 3b). A lower EPR intensity of the composite Si@Au NPs compared to the pure Si NPs can be associated with a decrease of disorder of the smaller NPs after laser-provoked structural modification. Moreover, they can also possess less defect states due to reduced amount of unpaired electrons caused by some “passivation” of silicon dangling bonds because of the silicon-gold interaction. Additional studies by XPS/XRD methods are required in order to establish the exact structure of composite nanoparticles and to prove the presence/absence of gold silicide

nanoformulations (Au_XSi_Y) of different stoichiometry. Nevertheless, no new kinds of paramagnetic defects related to Si–Au interaction or silicon oxidation are created.

Indeed, the estimation of the *g* factors reveals the same value for both types of NPs: $g_{Si@Au\ NPs}=g_{Si\ NPs}= 2.0055\pm0.0005$ that is related to silicon dangling bonds in amorphous silicon [55,56]. However, no silicon dangling bonds on the Si/SiO_2 interface (so-called P_b-centres) with anisotropic EPR signals (*g*-values around 2.002 and 2.008) are found for Si@Au NPs. Thus, laser-induced structural modification does not lead to the formation of a noticeable amount of any new types of defects detected by EPR. These data point out the identical mechanisms of interaction and subsequent aggregation of silicon nanoclusters regardless of the presence of gold nanoclusters.

The following hypothesis explaining the absence of any influence of optical as well as pulsed radio-frequency irradiation on the concentration of spins in Si-based NPs is suggested. As it is shown above, laser ablation leads to such extreme conditions as high temperature and pressure forming significantly inhomogeneous structure of both types of NPs. This synthesis can provoke the formation of some ensembles of defects due to their strong localisation in core of the NPs during the aggregation of the nanoclusters while surface defects may be passivated and thus become optically and radio-frequency inactive. Such a localisation may lead to very fast dissipation of energy of pulsed radio-frequency radiation due to strong spin-spin coupling that is confirmed by absence of any spin eco signal for both types of NPs in the temperature range between 20 and 300 K. These deeply localised defects are also insensitive to an optical excitation (532 nm) that is absorbed in a near-surface layer not influencing any paramagnetic defects inside the core. Another dissipation channel can be realised via strong interaction of NPs with the surrounding liquid environment. The presence of gold nanoclusters in the composite Si@Au NPs does not also influence the behaviour of the unpaired electrons in spite of resonant optical excitation leading to the formation of strong local electric fields. Insensitivity of unpaired electrons to resonant optical excitation in composite NPs indicates the absence of any plasmon-spin interactions.

Conclusions

Composite silicon-gold nanoparticles with several modalities are synthesized by pulsed laser ablation. Their size-distribution is significantly narrowed compared to that of initial silicon nanoparticles. Presence of both silicon and gold elements in composite nanoparticles is shown with mass contribution depended on their size. Remarkable plasmonic properties of Si-based nanoparticles are achieved in the whole visible range due to laser-induced structural modification. At the same time, expedient paramagnetic defect properties are also detected in them. Such nanoparticles may potentially serve as a novel revolutionary nanotool for nanomedicine simultaneously providing different actions (diagnostic, therapeutic, imaging, sensing).

Acknowledgements

This research work was financially supported from the European Regional Development Fund and the state budget of the Czech Republic (Project BIATRI: CZ.02.1.01/0.0/0.0/15_003/0000445), from the Ministry of Education, Youth and Sports (Programs NPU I-Project no. LO1602). Yu.V.R. also acknowledge a financial support from Freie Universität Berlin within the Excellence Initiative of the German Research Foundation (0503121810) as well as from a COST project (ECOST-STSM-BM1205-120416-072252).

Author contributions

Yu.V.R. conceived and designed the research, Yu.V.R. and J.B performed experiments, analysed obtained data and wrote the manuscript. All authors have given approval to the final version of the manuscript.

Figure Legends:

Figure 1. Composite Si-based nanoparticles: a) a TEM image of ensembles of NPs, b) a size distribution compared to that of initial Si NPs, c) a TEM image of 10 nm NP; d) a TEM image of 100 nm NP.

Figure 2. Structural properties of silicon-gold nanoparticles: a) an EDX spectrum of a 7 nm Si@Au NP, b) their size-dependent chemical composition.

Figure 3. Optical and electronic properties of silicon-gold nanoparticles: a) plasmonic properties of Si-based nanoparticles, b) electron paramagnetic resonance spectra of Si and Si@Au NPs in dark

(lines) and under green laser illumination (open points). Absorbance and double integral curves of Si@Au NPs are shown in inset.

Figure 4. A scheme of laser-induced formation of multifunctional Si-based nanoparticles (Si – silicon, Au – gold).

REFERENCES

[1] K.-Q. Peng, X. Wang, X.-L. Wu, S.-T. Lee, "Platinum Nanoparticle Decorated Silicon Nanowires for Efficient Solar Energy Conversion", *Nano Lett*, 2009, **9 (11)**, 3704–3709. https://doi.org/10.1021/nl901734e.

[2] J. Zhu, Z. Yu, G.F. Burkhard, C.-M. Hsu, S.T. Connor, Y. Xu, Q. Wang, M. McGehee, S. Fan, Y. Cui, "Optical Absorption Enhancement in Amorphous Silicon Nanowire and Nanocone Arrays", *Nano Lett*, 2009, **9 (1)**, 279–282. https://doi.org/10.1021/nl802886y.

[3] M.D. Kelzenberg, D.B. Turner-Evans, B.M. Kayes, M.A. Filler, M.C. Putnam, N.S. Lewis, H.A. Atwater, "Photovoltaic Measurements in Single-Nanowire Silicon Solar Cells", *Nano Lett*, 2008, **8 (2)**, 710–714. https://doi.org/10.1021/nl072622p.

[4] Y. Lu, Y. Yin, Z.-Y. Li, Y. Xia, "Synthesis and Self-Assembly of Au@SiO2 Core-Shell Colloids", *Nano Lett,* 2002, **2(7)**, 785–788. https://doi.org/10.1021/nl025598i.

[5] N. Kumar Pathak, N. Chander, V.K. Komarala, R.P. Sharma, "Plasmonic Perovskite Solar Cells Utilizing Au@SiO2 Core-Shell Nanoparticles, *Plasmonics*, 2016, **12**, 237–244. doi:10.1007/s11468-016-0255-9. https://doi.org/10.1007/s11468-016-0255-9.

[6] L. Hu, G. Chen, "Analysis of Optical Absorption in Silicon Nanowire Arrays for Photovoltaic Applications", *Nano Lett*, 2007, **7 (11)**, 3249–3252. https://doi.org/10.1021/nl071018b.

[7] Yu.V. Ryabchikov, V. Lysenko, T. Nychyporuk, "Enhanced Thermal Sensitivity of Silicon Nanoparticles Embedded in (nano-Ag)/SiNx for Luminescent Thermometry", *J Phys Chem C*, 2014, **118**, 12515–12519. https://doi.org/10.1021/jp411887s.

[8] Yu.V. Ryabchikov, S.A. Alekseev, V. Lysenko, G. Bremond, J-M. Bluet, "Photoluminescence thermometry with alkyl-terminated silicon nanoparticles dispersed in low-polar liquids", *Phys Status Solidi-R*, 2013, **7(6)**, 414–417. https://doi.org/10.1002/pssr.201307093.

[9] Yu.V. Ryabchikov, S.A. Alekseev, V. Lysenko, G. Bremond, J-M. Bluet, "Photoluminescence of silicon nanoparticles chemically modified by alkyl groups and dispersed in low-polar liquids", *J Nanopart Res*, 2013, **15(4)**, 1535–1–9. https://doi.org/10.1007/s11051-013-1535-3.

[10] Y. Cui, C.M. Lieber, "Functional Nanoscale Electronic Devices Assembled Using Silicon Nanowire Building Blocks", *Science*, 2001, **2915(5505)**, 851–853. https://doi.org/10.1126/science.291.5505.851.

[11] L.J. Chen, "Silicon nanowires: the key building block for future electronic devices", *J Mater Chem*, 2007, **17**, 4639–4643. https://doi.org/10.1039/B709983E.

[12] A.Yu. Kharin, V.V. Lysenko, A. Rogov, Yu.V. Ryabchikov, A. Geloen, I. Tishchenko, O. Marty, P.G. Sennikov, R.A. Kornev, I.N. Zavestovskaya, A.V. Kabashin, V.Yu. Timoshenko, "Bi-modal nonlinear

optical contrast from Si nanoparticles for cancer theranostics", *Adv Opt Mater*, 2019, **7(13)**, 18011728. https://doi.org/10.1002/adom.201801728.

[13] Z. Xu, X. Ma, Y.-E. Gao, M. Hou, P. Xue, C. M. Li, Y. Kang, "Multifunctional silica nanoparticles as a promising theranostic platform for biomedical applications", *Mater Chem Front*, 2017, **1**, 1257–1272. https://doi.org/10.1039/C7QM00153C.

[14] C.-C. Tu, K. Awasthi, K.-P. Chen, C.-H. Lin, M. Hamada, N. Ohta, Y.-K. Li, "Time-gated Imaging on Live Cancer Cells Using Silicon Quantum Dot Nanoparticles with Long-lived Fluorescence", *ACS Photonics*, 2017, **4(6)**, 1306–1315. https://doi.org/10.1021/acsphotonics.7b00188.

[15] J.-H. Park, L. Gu, G. von Maltzahn, E. Ruoslahti, S.N. Bhatia, M.J. Sailor, "Biodegradable luminescent porous silicon nanoparticles for *in vivo* applications", *Nat Mater*, 2009, **8**, 331–336. https://doi.org/10.1038/nmat2398.

[16] Yu.V. Ryabchikov, I.A. Belogorokhov, M.B. Gongalskiy, L.A. Osminkina, V.Yu. Timoshenko, "Photosensitized Generation of Singlet Oxygen in Powders and Aqueous Suspensions of Silicon Nanocrystals", *Semiconductors*, 2011, **45(8)**, 1059–1063. https://doi.org/10.1134/S106378261108015X.

[17] J. K. Lima, S. A. Majetich, "Composite magnetic – plasmonic nanoparticles for biomedicine: Manipulation and imaging", *Nano Today*, 2013, **8**, 98. https://doi.org/10.1002/pssa.200674306. 113. https://doi.org/10.1016/j.nantod.2012.12.010.

[18] Yu.V. Ryabchikov, I.A. Belogorokhov, A.S. Vorontsov, L.A. Osminkina, V.Yu. Timoshenko, P.K. Kashkarov, "Dependence of the Singlet Oxygen Photosensitization Efficiency on Morphology of Porous Silicon", *Phys Status Solidi A*, 2007, **204(5)**, 1271–1275. https://doi.org/10.1002/pssa.200674306.

[19] E.A. Konstantinova, V.A. Demin, A.S. Vorontzov, Yu.V. Ryabchikov, I.A. Belogorokhov, L.A. Osminkina, P.A. Forsh, P.K. Kashkarov, V.Yu. Timoshenko, "Electron Paramagnetic Resonance and Photoluminescence Study of Si Nanocrystals – Photosensitizers of Singlet Oxygen Molecules", *J Non-Cryst Solids*, 2006, **352(9-20)**, 1156-1159. https://doi.org/10.1016/j.jnoncrysol.2005.12.017.

[20] L. M. Bimbo, M. Sarparanta, H. A. Santos, A. J. Airaksinen, E. Makila, T. Laaksonen, L. Peltonen, V.-P. Lehto, J. Hirvonen, J. Salonen, "Biocompatibility of Thermally Hydrocarbonized Porous Silicon Nanoparticles and their Biodistribution in Rats", *ACS Nano*, 2010, **4(6)**, 3023–3032. https://doi.org/10.1021/nn901657w.

[21] F. Tang, L. Li, D. Chen, "Mesoporous Silica Nanoparticles: Synthesis, Biocompatibility and Drug Delivery", *Adv Mater*, 2012, **24**, 1504–1534. https://doi.org/10.1002/adma.201104763.

[22] N. O'Farrell, A. Houlton, B. R. Horrocks, "Silicon nanoparticles: applications in cell biology and medicine*", Int J Nanomedicine*, 2006, **1(4)**, 451–472.

[23] A. Detappe, E. Thomas, M.W. Tibbitt, S. Kunjachan, O. Zavidij, N. Parnandi, E. Reznichenko, F. Lux, O. Tillement, R. Berbeco, "Ultrasmall Silica-Based Bismuth Gadolinium Nanoparticles for Dual Magnetic Resonance−Computed Tomography Image Guided Radiation Therapy", *Nano Lett*, 2017, **17**, 1733−1740. https://doi.org/10.1021/acs.nanolett.6b05055.

[24] S.M. Hsiao, B.Y. Peng, Y.S. Tseng, H.T. Liu, C.H. Chen, H.M. Lin, "Preparation and characterization of multifunctional mesoporous silica nanoparticles for dual magnetic resonance and fluorescence imaging in targeted cancer therapy", *Micropor Mesopor Mat*, 2017, **250**, 210–220. https://doi.org/10.1016/j.micromeso.2017.04.050.

[25] I. Monaco, F. Arena, S. Biffi, E. Locatelli, B. Bortot, L. Cava, G.M. Marini, G.M. Severini, E. Terreno, M.C. Franchini, "Synthesis of Lipophilic Core−Shell Fe3O4@SiO2@Au Nanoparticles and Polymeric Entrapment into Nanomicelles: A Novel Nanosystem for in Vivo Active Targeting and Magnetic Resonance−Photoacoustic Dual Imaging", *Bioconjugate Chem*, 2017, **28**, 1382−1390. https://doi.org/10.1021/acs.bioconjchem.7b00076.

[26] K. Stockhofe, J.M. Postema, H. Schieferstein, T.L. Ross, "Radiolabeling of Nanoparticles and Polymers for PET Imaging", *Pharmaceuticals*, 2014, **7**, 392−418. https://doi.org/10.3390/ph7040392.

[27] A. Srivatsan, X. Chen, "Recent Advances in Nanoparticle-Based Nuclear Imaging of Cancers", *Adv Cancer Res*, 2014, **124**, 83−129. https://doi.org/10.1016/B978-0-12-411638-2.00003-3.

[28] J.C. Gore, H.C. Manning, C.C. Quarles, K.W. Waddell, T.E. Yankeelov, "Magnetic resonance in the era of molecular imaging of cancer", *Magn Reson Imaging*, 2011, **29**, 587–600. https://doi.org/10.1016/j.mri.2011.02.003.

[29] J. Kim, H.S. Kim, N. Lee, T. Kim, H. Kim, T. Yu, I.C. Song, W.K. Moon, T. Hyeon, "Multifunctional Uniform Nanoparticles Composed of a Magnetite Nanocrystal Core and a Mesoporous Silica Shell for Magnetic, Resonance and Fluorescence Imaging and for Drug Delivery", *Angew Chem Int Ed*, 2008, **47**, 8438–8441. https://doi.org/10.1002/anie.200802469.

[30] A. Al–Kattan, Yu.V. Ryabchikov, T. Baati, V. Chirvony, J.F. Sanchez–Royo, M. Sentis, D. Braguer, V.Yu. Timoshenko, M.–A. Estève, A.V. Kabashin, "Ultrapure laser–synthesized Si nanoparticles with variable oxidation state for biomedical applications", *J Mater Chem B*, 2016, **4**, 7852–7858. https://doi.org/10.1039/C6TB02623K.

[31] Yu.V. Ryabchikov, "Size Modification of Optically Active Contamination-Free Silicon Nanoparticles with Paramagnetic Defects by Their Fast Synthesis and Dissolution", *Phys Status Solidi A*, 2019, **216(2)**, A1800685. https://doi.org/10.1002/pssa.201800685.

[32] Yu.V. Ryabchikov, A. Al–Kattan, V. Chirvony, J.F. Sanchez–Royo, M. Sentis, V.Yu. Timoshenko, A.V. Kabashin, "Influence of oxidation state on water solubility of Si nanoparticles prepared by laser ablation in water", *Proc SPIE*, 2017, **10078**, 100780C–1–7. https://doi.org/10.1117/12.2257404.

[33] S.N. Voicu, M. Balas, M.S. Stan, B. Trică, A.I. Serban, L. Stanca, A. Hermenean, A. Dinischiotu, "Amorphous Silica Nanoparticles Obtained by Laser Ablation Induce Inflammatory Response in Human Lung Fibroblasts", *Materials*, 2019, **12(7)**, 1026. https://doi.org/10.3390/ma12071026.

[34] M. Qiu, A. Singh, D. Wang, J. Qu, M. Swihart, H. Zhang, P.N. Prasad, "Biocompatible and biodegradable inorganic nanostructures for nanomedicine: Silicon and black phosphorus", *Nano Today*, 2019, **25**, 135–155. https://doi.org/10.1016/j.nantod.2019.02.012.

[35] N.A. Smirnov, S.I. Kudryashov, A.A. Nastulyavichus, A.A. Rudenko, I.N. Saraeva, E.R. Tolordava, S.A. Gonchukov, Yu.M. Romanova, A.A. Ionin, D.A. Zayarny, "Antibacterial properties of silicon nanoparticles", *Laser Phys Lett*, 2018, **15**, 105602. https://doi.org/10.1088/1612-202X/aad853.

[36] Yu.V. Ryabchikov, "Facile Laser Synthesis of Multimodal Composite Silicon/Gold Nanoparticles with Variable Chemical Composition", *J Nanopart Res*, 2019, **21(4)**, 85. https://doi.org/10.1007/s11051–019–4523–4.

[37] Yu.V. Ryabchikov, A.A. Popov, M. Sentis, V.Yu. Timoshenko, A.V. Kabashin, "Structural properties of gold-silicon nanohybrids formed by femtosecond laser ablation in water at different fluences", *Proc SPIE*, 2016, **9737**, 97370F–1–6. https://doi.org/10.1117/12.2217777.

[38] I.N. Saraeva, N.V. Luong, S.I. Kudryashov, A.A. Rudenko, R.A. Khmelnitskiy, A.L. Shakhmin, A.Y. Kharin, A.A. Ionin, D.A. Zayarny, D.H. Tung, P.V. Duong, P.H. Minh, "Laser synthesis of colloidal Si@Au and Si@Ag nanoparticles in water via plasma-assisted reduction", *J Photoch Photobio A*, 2018, **360**, 125-131. https://doi.org/10.1016/j.jphotochem.2018.04.004.

[39] P. Nasiri, D. Doranian, A.H. Sari, "Synthesis of Au/Si nanocomposite using laser ablation method", *Opt Laser Technol*, 2019, **113**, 217-224. https://doi.org/10.1016/j.optlastec.2018.12.033.

[40] Y. Yoshida, S. Watanabe, Y. Nishijima, K. Ueno, H. Misawa and T. Kato, "Fabrication of a Au/Si nanocomposite structure by nanosecond pulsed laser irradiation", *Nanotechnology*, 2011, **22**, 375607. https://doi.org/10.1088/0957-4484/22/37/375607.

[41] P. B. Tan, K. Venkatakrishnan, "Ultrafast laser functionalized rare phased gold–silicon/silicon oxide nanostructured hybrid biomaterials", *Colloid Surface B*, 2015, **136**, 828–837. https://doi.org/10.1016/j.colsurfb.2015.10.007.

[42] R. Riedel, N. Mahr, C. Yao, A. Wu, F. Yang and N. Hampp, "Synthesis of gold–silica core–shell nanoparticles by pulsed laser ablation in liquid and their physico-chemical properties towards photothermal cancer therapy", *Nanoscale*, 2020, **12**, 3007-3018. https://doi.org/10.1039/C9NR07129F.

[43] P. Pingel, M. Arvind, L. Kölln, R. Steyrleuthner, F. Kraffert, J. Behrends, S. Janietz, D. Neher, "p-Type Doping of Poly(3-hexylthiophene) with the Strong Lewis Acid Tris(pentafluorophenyl)borane", *Adv Electron Mater*. 2016, **2**, 1600204. https://doi.org/10.1002/aelm.201600204.

[44] T. Donnelly, J.G. Lunney, S. Amoruso, R. Bruzzese, X. Wang, X. Ni, "Dynamics of the plumes produced by ultrafast laser ablation of metals", *J Appl Phys*, 2010, **108**, 043309. https://doi.org/10.1063/1.3475149.

[45] A. Semerok, B. Salle, J.-F. Wagner, G. Petite, "Femtosecond, picosecond, and nanosecond laser microablation: Laser plasma and crater investigation Laser and Particle Beams", *Laser Part Beams*, 2002, **20**, 67–72. https://doi.org/10.1017/S0263034602201093.

[46] S.S. Harilal, J.R. Freeman, P.K. Diwakar, A. Hassanein. (2014) Femtosecond Laser Ablation: Fundamentals and Applications. In: Musazzi S., Perini U. (eds) Laser-Induced Breakdown Spectroscopy. Springer Series in Optical Sciences, vol 182. Springer, Berlin, Heidelberg.

[47] H. Zeng, X.-W. Du, S.C. Singh, S.A. Kulinich, S. Yang, J. He, W. Cai, "Nanomaterials via Laser Ablation/Irradiation in Liquid: A Review", *Adv Funct Mat*, 2012, **22**, 133–1353. https://doi.org/10.1002/adfm.201102295.

[48] D. Tan, S. Zhou, J. Qiu, N. Khusro, "Preparation of functional nanomaterials with femtosecond laser ablation in solution", *J Photoch Photobio C*, 2013, **17**, 50–68. http://doi.org/10.1016/j.jphotochemrev.2013.08.002.

[49] G.W. Yang, "Laser ablation in liquids: Applications in the synthesis of nanocrystals*", Prog Mater Sci*, 2007, **52**, 648–698. http://doi.org/10.1016/j.pmatsci.2006.10.016.

[50] K.C. Phillips, H.H. Gandhi, E. Mazur, S.K. Sundaram, "Ultrafast laser processing of materials: a review", *Adv Opt Photonics*, 2015, **7(4)**, 684–712. http://doi.org/10.1364/AOP.7.000684.

[51] H. Zeng, X.W. Du, S.C. Singh, S.A. Kulinich, S. Yang, J. He, W. Cai, "Nanomaterials via laser ablation/irradiation in liquid: a review", *Adv Func Mat*, 2012, **22(7)**, 1333-1353. https://doi.org/10.1002/adfm.201102295

[52] S. Ibrahimkutty, P. Wagener, A. Menzel, A. Plech and S. Barcikowski, "Nanoparticle formation in a cavitation bubble after pulsed laser ablation in liquid studied with high time resolution small angle x-ray scattering", *Appl Phys Lett*, 2012, **101**, 103104. http://dx.doi.org/10.1063/1.4750250.

[53] E. Boulais, R. Lachaine, A. Hatef, M.Meunier, "Plasmonics for pulsed-laser cell nanosurgery: Fundamentals and applications", *J Photoch Photobio C*, 2013, **17**, 26-49. https://doi.org/10.1016/j.jphotochemrev.2013.06.001.

[54] C.-Y. Shih, M.V. Shugaev, C. Wu, L.V. Zhigilei, "Generation of subsurface voids, incubation effect, and formation of nanoparticles in short pulse laser interactions with bulk metal targets in liquid: molecular dynamics study", *J Phys Chem C*, 2017, **121**, 30, 16549-16567. https://doi.org/10.1021/acs.jpcc.7b02301.

[55] A. Couairona, A. Mysyrowicz, "Femtosecond filamentation in transparent media", *Phys Rep*, 2007, **441(2–4)**, 47-189. https://doi.org/10.1016/j.physrep.2006.12.005.

[56] M. Baran, B. Bulakh, N. Korsunska, L. Khomenkova, J. Jedrzejewski, "Luminescence and EPR studies of defects in Si–SiO_2 films", *Eur Phys J-Appl Phys*, 2004, **27**, 285–287. http://doi.org/10.1051/epjap:2004089.

[57] M. Shimasaki, Y. Show, M. Iwase, T. Izumi, T. Ichinohe, S. Nozaki, H. Morisaki, "Correlation between light emission and dangling bonds in porous silicon", *Appl Surf Sci*, 1996, **92(2)**, 617–620. http://doi.org/10.1016/0169-4332(95)00304-5.

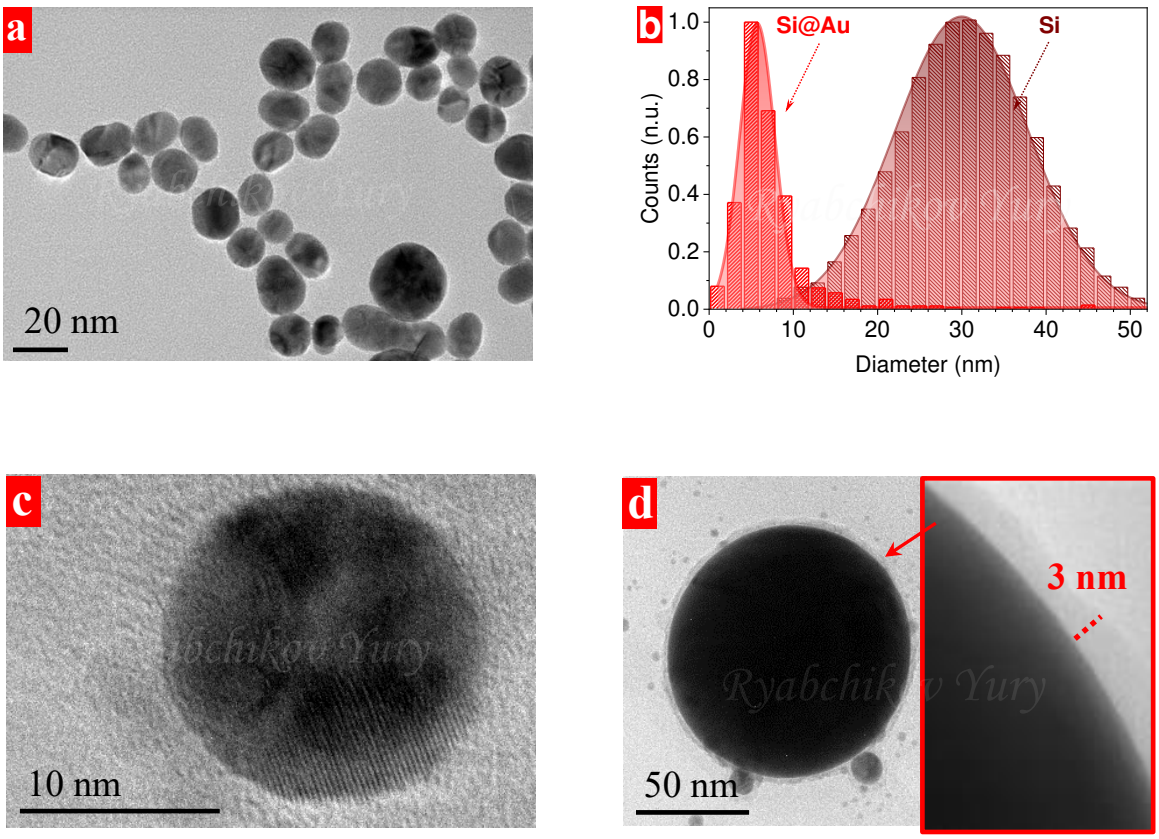

Figure 1. Composite Si-based nanoparticles: a) a TEM image of ensembles of NPs, b) a size distribution compared to that of initial Si NPs, c) a TEM image of 10 nm NP; d) a TEM image of 100 nm NP.

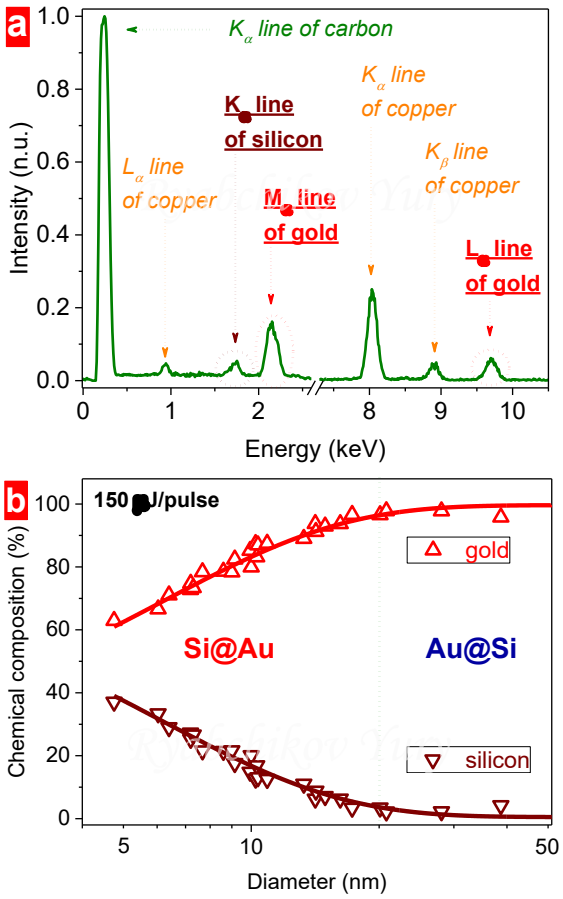

Figure 2. Structural properties of silicon-gold nanoparticles: a) an EDX spectrum of a 7 nm Si@Au NP, b) their size-dependent chemical composition (mass ratio).

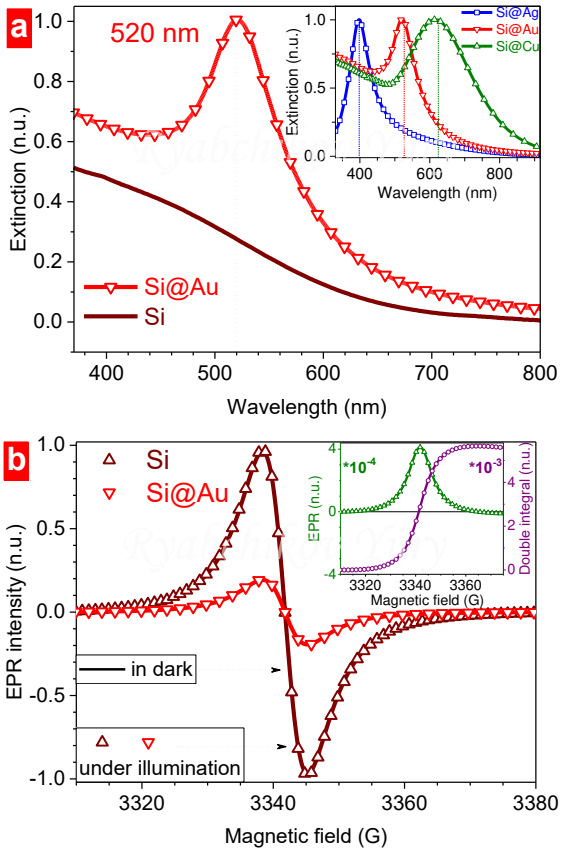

Figure 3. Optical and electronic properties of silicon-gold nanoparticles: a) plasmonic properties of Si-based nanoparticles, b) electron paramagnetic resonance spectra of Si and Si@Au NPs in dark (lines) and under green laser illumination (open triangles). Absorbance and double integral curves of Si@Au NPs are shown in inset.

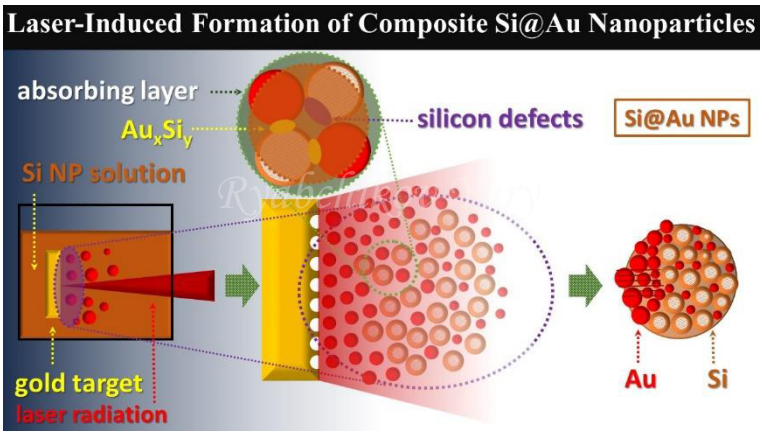

Figure 4. A scheme of laser-induced formation of multifunctional Si-based nanoparticles (Si – silicon, Au – gold).